
Article

Not peer-reviewed version

Modelling the Dynamics of a Wheeled Mobile Robot System Using a Hybridisation of Fuzzy Linear Quadratic Gaussian

[Sairoel Amertet Finecomess](#) ^{*}, [Girma Gebresenbet](#), Hassan Mohammed Alwan

Posted Date: 21 June 2024

doi: [10.20944/preprints202406.1465.v1](https://doi.org/10.20944/preprints202406.1465.v1)

Keywords: wheeled mobile robot; optimisation; position; orientation; Lorenz law of attraction



Preprints.org is a free multidiscipline platform providing preprint service that is dedicated to making early versions of research outputs permanently available and citable. Preprints posted at Preprints.org appear in Web of Science, Crossref, Google Scholar, Scilit, Europe PMC.

Copyright: This is an open access article distributed under the Creative Commons Attribution License which permits unrestricted use, distribution, and reproduction in any medium, provided the original work is properly cited.

Disclaimer/Publisher's Note: The statements, opinions, and data contained in all publications are solely those of the individual author(s) and contributor(s) and not of MDPI and/or the editor(s). MDPI and/or the editor(s) disclaim responsibility for any injury to people or property resulting from any ideas, methods, instructions, or products referred to in the content.

Article

Modelling the Dynamics of a Wheeled Mobile Robot System Using a Hybridisation of Fuzzy Linear Quadratic Gaussian

Sairoel Amertet Finecomess ^{1,*}, Girma Gebresenbet ² and Hassan Mohammed Alwan ¹

¹ High School of Automation and Robotics, Peter the Great Saint Petersburg Polytechnic University, 195220 Saint Petersburg, Russia, sairoel@mtu.edu.et

² Department of Energy and Technology, Swedish University of Agricultural Sciences, P.O. Box 7032, 750 07 Uppsala, Sweden, girma.gebresenbet@slu.se

* Correspondence: sairoel@mtu.edu.et

Abstract: Wheeled mobile robot dynamics and suitable controller design are challenging but rewarding fields of study. By understanding the dynamics of wheeled mobile robots, it could be possible to design suitable hybrid control schemes for wheeled mobile robots. Since hybrid control schemes involve combining individual control methods to create a more effective overall control strategy. This can be done in a variety of ways, such as using fuzzy linear quadratic Gaussian control. We were therefore inspired to create dynamic models and their controller designs for the wheeled mobile robot by examining the dynamics of the wheeled mobile robot. The novelty of the current paper is to hybridize the different control schemes for wheeled mobile robots in order to get better performance. Entire systems models were simulated in a MATLAB/SIMULINK environment. The results obtained for the settling time response by FLQG were 87.1% over LQG; this study compared the effectiveness of current and previous FLQG controllers in external disturbances and found peak amplitude improvements of 71.25%. Therefore, the proposed controller is suitable for use with the wheeled mobile robot.

Keywords: wheeled mobile robot; optimisation; position; orientation; Lorenz law of attraction

1. Introduction

Inequalities in global food supply have left 821 million people undernourished, according to the Food and Agriculture Organization (FAO) [1]. The introduction of sophisticated technology is key to feeding the world's population, and can help simplify solutions to meeting the world's food needs. Wheeled mobile robots are an example of such cutting-edge technologies [2]. Agriculture-related industries make extensive use of wheeled mobile robot systems (WMRS). Over the past thirty years, there has been ongoing research on, and development of, wheeled mobile robots (WMRs) [3]. The primary driving force behind this sustained interest has been the multitude of real-world uses that mobile robots can provide because of their adaptability to operating in vast, potentially dangerous and unstructured environments. In particular [4–6], WMRs have been used in munitions handling, material transportation, vacuum cleaners, entertainment, industry, hospitals, education, rescue, mine detection, monitoring of nuclear facilities and warehouses for material inspection and security objectives, and planetary exploration [7]. It is evident from this list of its many applications that WMR research is, by its very nature, multidisciplinary. Numerous scholars have devised techniques for the kinematic and dynamic simulation of mobile robots on wheels. A thorough investigation of this topic was undertaken by [8]. Specifically, kinematic modelling and dynamic modelling – which are similar to those of stationary robot manipulators – lack a consistent formulation. Kinematic and dynamic modelling is well-established in the literature on wheeled mobile robots; for example, kinematic models are obtained by coordinate transformations, while dynamic models are obtained using

Lagrange and Newton-Euler. Therefore, a combination of the two approaches with mobile robots will be the subject of future research to bring together the two disparate literatures. This work to develop dynamic models of the mobile robot was motivated by studies of the dynamics of the wheeled mobile robot. Although the methodologies differ, the outcome of this work is presented in a manner similar to that of [9,10]. The skid-steering mobile robot (SSMR) model was used to define wheel dynamics, Lagrangian was used to derive the mobile robot's dynamics, and fuzzy logic linear quadratic Gaussian (LQG) controllers were proposed to regulate and robustly control the wheeled mobile robotic dynamic. Examination of a Jacobian matrix is the primary method used by researchers to quantify the kinematic performance of a robotic kinematic [11]. Conversely, dynamic performance can be defined as the wheel's perceived acceleration capability of the actuators or of the wheel itself [12]. In robotics literature, less attention has been paid to the dynamics analysis of mobile robots [13–16]. Using the methodologies from the dynamics of wheeled mobile robotics to analyse the performance of mobile robots is the next step in achieving an optimal design. The dynamic model of the wheel is formulated as a skidding mobile robot system. Finally, the theorem of the Lorenz system was formulated and analysed in relation to the WMRS controller framework. The remainder of this paper is arranged as follows: section 2 describes the literature reviews, section 3 presents the mathematical models and control theory design applied in the development of the model, and section 4 describes and discusses the modelling outcomes. Conclusions from the study are presented in section 5.

2. Literature Review

Wheeled and legged robots are the main categories of mobile robots. Legged robots have an edge on uneven terrain and are faster on smooth surfaces, while wheeled mobile robots (WMRs) are more energy-efficient and easier to construct, making them suitable for potential industry applications. However, multi-joint limb actuation is more complex. The work of [17–19] aims to optimise a control system algorithm for robotic assets using a multi-generic decision-making technique, focusing on internal actions within the system, to determine the best robotic system for agricultural monitoring tasks. The study proposes an adaptive control method using reinforcement learning to solve the nonlinear state tracking problem and input time delay system in wheeled mobile robots [20]. It presents a delay matrix function and Lyapunov functionals, and defines adaptive laws for the controller and critic neural networks. A discrete-time linear-quadratic regulator with integral control, known as an LQR predictive controller, was developed for MIMO time-delay processes, successfully treating large, non-minimum phase modes and integrating stable and unstable output anomalies at random.

Model predictive control (MPC) is an advanced control algorithm that uses a model of the plant to predict future behaviour and optimise control actions. While MPC offers many advantages, there are also some drawbacks associated with its use in a wheeled mobile robot, such as **computational complexity, model accuracy, sensitivity to disturbances, limited handling of constraints and tuning complexity** [21–23]. Adaptive MPC is an advanced control technique that has attracted significant attention in recent years due to its ability to handle complex systems with uncertainties and time-varying parameters. However, like any control technique, adaptive MPC also has certain drawbacks that should be considered when using it in wheeled mobile robot applications. These drawbacks are **increased computational complexity, sensitivity to noise and disturbances, limited convergence rate, potential overfitting and the requirement for persistent excitation** [24].

In order to alter the behaviour of systems by leveraging past outputs to affect future inputs, feedback control is a commonly utilised technique in engineering and other domains [25,26]. When applied to mobile robot dynamics, feedback control systems have many benefits, but they also have certain disadvantages, including time delay, instability, noise amplification, complexity and expense. Systems with unknown dynamics can be controlled using nonlinear control techniques such as sliding mode control. Although it has a number of benefits, including resistance to disturbances and changes in parameters, it also has some disadvantages that restrict its use in specific situations. High control effort, chattering, sensitivity to noise, low bandwidth, implementation difficulty and a lack of

robustness to unmodelled dynamics are examples of such shortcomings [27–29]. In variable structure control systems, super slide mode control is a technique that enhances a system's robustness and performance. Its foundation is the concept of creating a sliding surface in the system's state space and then creating a control law that compels the system to move along it. However, it can also cause a chattering phenomenon: when the system state quickly flips between the two sides of the sliding surface, chattering occurs. In certain wheeled mobile robot applications, this might result in high-frequency oscillations in the control signal, which is undesirable. Stability is possible with super slide mode control, but if the sliding surface is not appropriately engineered, the system could behave erratically and become unstable.

Convolutional neural networks do not require human supervision for image classification and identifying important features in images [30]. However, when applied in wheeled mobile robotic dynamics, the system is faced with the following problems: high computational requirements, a large amount of labelled data, a large memory footprint, interpretability challenges, limited effectiveness for sequential data, a tendency to be much slower, and a requirement for extensive training [31].

A proportional integral derivative (PID) controller is a control mechanism widely used in various industries to regulate processes and maintain desired outputs [32]. While PID controllers offer numerous advantages, they have certain drawbacks that limit their effectiveness in certain scenarios. These include **limited performance in nonlinear systems, sensitivity to noise and disturbances, integral windup, derivative kick, tuning complexity and limited adaptability**.

A fuzzy PID controller combines the principles of fuzzy logic and PID control to enhance the performance of control systems. While it offers several benefits, there are certain disadvantages associated with its use. These are **computational complexity, tuning difficulty, a lack of an analytical framework, limited adaptability and knowledge dependency**. Despite these drawbacks, fuzzy PID controllers remain a valuable tool in certain applications, particularly when dealing with complex nonlinear systems where traditional control techniques may not be applicable [33].

The PID-LQR controller is a control algorithm that is widely used in various industries. However, like any control technique, it has certain drawbacks that should be considered in its implementation. It is sensitive to model uncertainties, the controller is heavily reliant on an accurate mathematical model of the plant or system being controlled, and if the model is not accurate or if there are significant disturbances or unmodelled dynamics, the controller's performance can deteriorate or even become unstable. Furthermore, the PID-LQR controller requires careful tuning of its parameters to achieve optimal performance. This tuning process can be challenging and time-consuming, requiring expertise in control theory and a deep understanding of the system being controlled [34].

A proportional integral derivative linear quadratic Gaussian (PID-LQG) controller is a control algorithm that combines the benefits of PID control with the optimal control theory of LQG. While PID control is simple and widely used, it can be limited in its ability to handle complex systems and disturbances. LQG control, however, provides a more systematic approach to controller design, but can be computationally expensive and requires a detailed model of the system. Fuzzy LQR (FLQR) control is a control technique that combines the advantages of fuzzy logic and linear-quadratic regulator (LQR) control. However, like any control technique, FLQR control has its drawbacks. Nevertheless, it remains a powerful technique for controlling linear and nonlinear systems. It offers a systematic approach to controller design and can provide excellent performance when the system model is accurate and the disturbances are limited. In terms of performance, it has very promising applications with the wheeled mobile robot in order to achieve excellent regulation and robustness [35,36].

3. Dynamic Models and the Controller Design of a Wheeled Mobile Robot

3.1. Development of a Kinematic Model of a Four-Wheeled Mobile Robot for Agricultural Applications

Case study and assumptions

Assumptions in dynamic model development are principles, simplifications and approximations that make the model tractable and computationally feasible, while capturing real-

world system characteristics. Common assumptions depend on the model's nature and modelling objectives [8]. The importance of assumptions in wheeled mobile robot model design lies in their ability to simplify the problem, capture the essential characteristics, enable analysis and simulation, facilitate design decisions, assess the model's limitations, and enable comparisons and benchmarking. Careful consideration of these assumptions is crucial for developing accurate and reliable models that can guide the design and development of effective wheeled mobile robots. The assumptions in this study were:

- **linearity:** assuming that the system behaves in a linear manner, where the output is directly proportional to the input, this simplifies the mathematical analysis and allows for the use of linear techniques
- **time-invariance:** assuming that the system's behaviour does not change over time, this means that the system's properties and characteristics remain constant throughout the modelling period
- **homogeneity:** assuming that the system's behaviour is uniform throughout its spatial domain, this means that the system's properties and characteristics are the same at all points in space
- **determinism:** assuming that the system's behaviour is fully determined by its initial conditions and inputs, this excludes the influence of random or stochastic factors
- **perfect knowledge:** assuming that all relevant information about the system is known and available for modelling purposes, this includes complete knowledge of the system's structure, parameters and boundary conditions.

Agriculture, a major economic sector, contributes 6.4 % of global productivity and employs a significant workforce. In view of concerns about food security, population growth and climate change, innovative approaches such as wheeled mobile robots are being explored. Figure 1 shows a wheeled mobile robot in use in agricultural areas. This wheeled mobile is dynamic since it observes the entire plant's health status as it moves along.



Figure 1. A wheeled mobile robot in dynamic action in the field [8].

Following the literature review, kinematical models of a wheeled mobile robot were developed (Figure 2). Based on the kinematical models of a wheeled mobile robot, state space was generated. The kinematical models of wheeled mobile robots then required regulation, and the optimal controllers were selected for this. If the gain obtained was optimal, it was directly provided to the dynamical models of the wheeled mobile robot. Subsequently, data were collected from the dynamic

models of the wheeled mobile robot for analysis purposes. If the gain was not optimal, the controller design was examined again, with the tuned and relaunched system checked until the desired optimal gain was obtained.

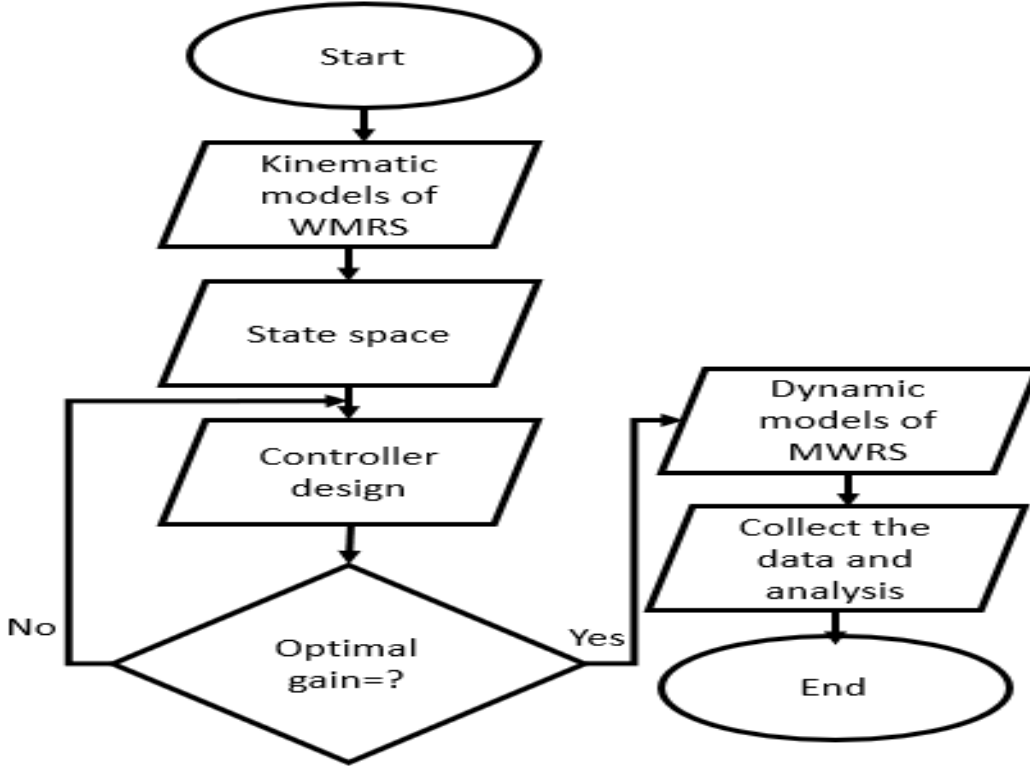


Figure 2. Scheme for the present work.

Considering only the kinematic equation model of the SSMR (Figure 3), the following velocity constraint was obtained:

$$v_y + x_{ICR}\dot{\theta} = 0 \quad (1)$$

Where x_{ICR} is inertia centre, v_y is vertical velocity of the robot, and $\dot{\theta}$ is angular velocity of the mobile robot.

Equation (1) is not integrable and is consequently a nonholonomic constraint. It can therefore be rewritten in the form $[-\sin\theta \cos\theta x_{ICR}] [\dot{x} \dot{y} \dot{\theta}] = A(q)\dot{q} = 0$, where equation (1) is used. Since the generalised velocity is always in the null space of A, the last equation is not integrable. Consequently, it describes a nonholonomic constraint that can be rewritten in the Pfaffian form:

$$[-\sin\theta \cos\theta x_{ICR}] [\dot{X} \dot{Y} \dot{\theta}] = A(q)\dot{q} = 0 \quad (2)$$

$$\dot{q} = S(q)\eta \quad (3)$$

Where $S(q)\eta$ is state space variable matrix.

Rearranging the kinematics models, the state space equation below was finally achieved:

$$S(q) = \begin{bmatrix} \cos\theta & x_{ICR} \sin\theta \\ \sin\theta & -x_{ICR} \cos\theta \end{bmatrix} \quad (4)$$

The input matrix is the following equation:

$$\beta = \begin{bmatrix} V_x \\ \omega \end{bmatrix} = r \begin{bmatrix} \frac{\omega_L + \omega_R}{2} \\ \frac{-\omega_L + \omega_R}{2c} \end{bmatrix} \quad (5)$$

Where β is velocity vectors of both linear and angular velocity.

Then the dynamic properties of the SSMR were described, since the dynamic effects play an important role in such vehicles. This is caused by unknown lateral skidding ground interaction forces. First, the wheel forces depicted in Figure 3 were examined.

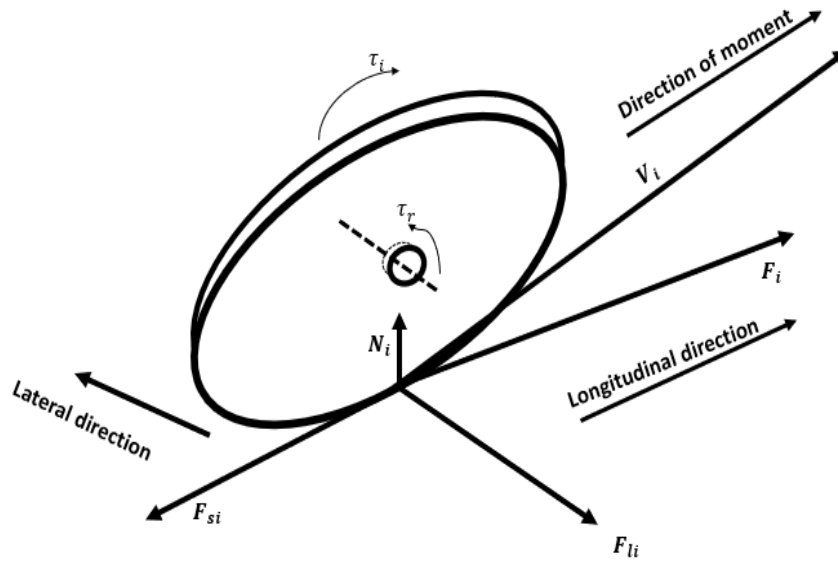


Figure 3. Forces acting on one wheel [8].

The active force F_i and reactive force N_i are related to the wheel torque and gravity, respectively. It is clear that F_i is linearly dependent on the wheel control input τ_i , namely:

$$F_i = \frac{\tau_i}{r} \quad (6)$$

It was assumed that the vertical force N_i acts from the surface to the wheel. Considering the four wheels of the vehicle (Figure 4) and neglecting additional dynamic properties, the following equations of equilibrium were obtained:

$$\begin{cases} N_1 a = N_2 b \\ N_3 a = N_4 b \\ \sum_{i=1}^4 N_i = mg \end{cases} \quad (7)$$

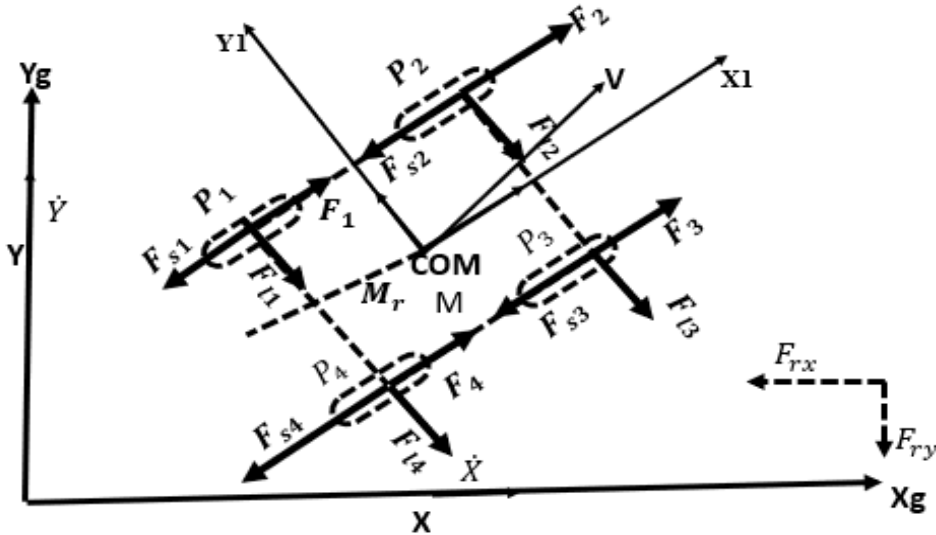


Figure 4. Active and resistive forces of the vehicle [8].

where m denotes the vehicle mass and g is the gravity acceleration. Where p_1, p_2, p_3, p_4 are the position of robot wheels, $F_1, F_2, F_3, F_4, F_{s1}, F_{s2}, F_{s3}, F_{s4}, F_{l1}, F_{l2}, F_{l3}, F_{l4}$, are forces on the wheels, M

moment of the wheels, τ_r, τ_i , torques of the wheels V_i velocities of the wheel, V velocity of the mobile robot. Since there is symmetry along the longitudinal midline, the following was obtained:

$$\begin{cases} N_1 = N_4 = \frac{b}{2(a+b)} mg \\ N_2 = N_3 = \frac{a}{2(a+b)} mg \end{cases} \quad (8)$$

It was assumed that the vector F_{si} results from the rolling resistant moment τ_{ri} and the vector F_{li} denotes the lateral reactive force. These reactive forces can be regarded as friction forces. However, it is important to note that friction modelling is quite complicated since it is highly nonlinear and depends on many variables. Therefore, in most cases only a simplified approximation describing the friction F_f as a superposition of Coulomb and viscous friction is considered. It can be written as:

$$F_f(\sigma) = \mu_c N \operatorname{sgn}(\sigma) + \mu_v \sigma \quad (9)$$

where σ denotes the linear velocity, N is the force perpendicular to the surface, and μ_c and μ_v denote the coefficients of Coulomb and viscous friction, respectively. Since for the SSMR the velocity σ is relatively low, especially during lateral slippage, the relation $\mu_c N \gg |\mu_v \sigma|$ is valid, which allowed the term $\mu_v \sigma$ to be neglected to simplify the model. It is very important to note that the function of a kinematics system is not smooth when the velocity σ equals zero, because of the sign function $\operatorname{sgn}(\sigma)$. It is obvious that this function is not differentiable at $\sigma = 0$. Since the aim was to obtain a continuous and time-differentiable model of the SSMR, the following approximation of this function was proposed:

$$\widehat{\operatorname{sgn}}(\sigma) = \frac{2}{\pi} \arctan(k_s \sigma) \quad (10)$$

where $k_s \gg 1$ is a constant that determines the approximation accuracy according to the relation

$$\lim_{n \rightarrow \infty} \frac{2}{\pi} \arctan(k_s \sigma) = \operatorname{sgn}(\sigma) \quad (11)$$

Based on the previous deliberations, the friction forces for one wheel can be written as:

$$F_{li} = \mu_{lci} m g \widehat{\operatorname{sgn}}(v_{yi}) \quad (12)$$

$$F_{si} = \mu_{sci} m g \widehat{\operatorname{sgn}}(v_{xi}) \quad (13)$$

where μ_{lci} and μ_{sci} denote the coefficients of the lateral and longitudinal forces, respectively. Using the Lagrange-Euler formula with Lagrange multipliers to include the nonholonomic constraint (1), the dynamic equation of the robot can be obtained. Next, it was assumed that the potential energy of the robot $P E(q) = 0$ because of the planar motion. Therefore, the Lagrangian L of the system equals the kinetic energy:

$$L(q, \dot{q}) = T(q, \dot{q}) \quad (14)$$

Considering the kinetic energy of the vehicle and neglecting the energy of rotating wheels, the following equation was developed:

$$T = \frac{1}{2} m v^T v + \frac{1}{2} I \omega^2 \quad (15)$$

where m denotes the mass of the robot and I is the moment of inertia of the robot about the COM. For simplicity, it was assumed that the mass distribution is homogeneous. Since

$$v^T v = v_x^2 + v_y^2 = \dot{X}^2 + \dot{Y}^2 \quad (16)$$

substituting equation (16) into eqn. (15) can be rewritten in the following form:

$$T = \frac{1}{2} m (\dot{X}^2 + \dot{Y}^2) + \frac{1}{2} I \dot{\theta}^2 \quad (17)$$

After calculating the partial derivative of kinetic energy and its time derivative, the inertial forces could be obtained as

$$\frac{d}{dt} \left(\frac{\partial E_k}{\partial \dot{q}} \right) = \begin{bmatrix} m \ddot{X} \\ m \ddot{Y} \\ I \ddot{\theta} \end{bmatrix} = M \ddot{q} \quad (18)$$

where

$$M = \begin{bmatrix} m & 0 & 0 \\ 0 & m & 0 \\ 0 & 0 & m \end{bmatrix} \quad (19)$$

Consequently, the forces that cause the dissipation of energy were considered. In accordance with Figure 2, the following resultant forces expressed in the inertial frame could be calculated:

$$F_{ry}(\dot{q}) = \cos\theta \sum_{i=1}^4 F_{si}(v_{xi}) - \sin\theta \sum_{i=1}^4 F_{li}(v_{yi}) \quad (20)$$

$$F_{ry}(\dot{q}) = \sin\theta \sum_{i=1}^4 F_{si}(v_{xi}) + \cos\theta \sum_{i=1}^4 F_{li}(v_{yi}) \quad (21)$$

The resistant moment around the centre of mass M_r can be obtained as

$$\begin{cases} M_r(\dot{q}) = -a \sum_{i=1,4} F_{li}(v_{yi}) + b \sum_{i=2,4} F_{li}(v_{yi}) \\ \quad + c \left[- \sum_{i=1,2} F_{si}(v_{xi}) + \sum_{i=3,4} F_{si}(v_{xi}) \right] \end{cases} \quad (22)$$

To define generalised resistive forces, the vector

$$R(\dot{q}) = [F_{rx}(\dot{q}) \ F_{ry}(\dot{q}) \ M_r(\dot{q})]^T \quad (23)$$

was introduced. The active forces generated by the actuators which make the robot move can be expressed in the inertial frame as follows:

$$F_x = \cos\theta \sum_{i=1}^4 F_i \quad (24)$$

$$F_y = \sin\theta \sum_{i=1}^4 F_i \quad (25)$$

The active torque around the common point was calculated as:

$$M = c(-F_1 - F_2 + F_3 + F_4) \quad (26)$$

Consequently, the vector F of active forces had the following form:

$$F = [F_x \ F_y \ M]^T \quad (27)$$

Using (4), (26) and (27) and assuming that the radius of each wheel is the same, this gave

$$F = \frac{1}{r} \begin{bmatrix} \cos\theta \sum_{i=1}^4 \tau_i \\ \sin\theta \sum_{i=1}^4 \tau_i \\ c(-\tau_1 - \tau_2 + \tau_3 + \tau_4) \end{bmatrix} \quad (28)$$

To simplify the notation, a new torque control input τ was defined as

$$\tau = \begin{bmatrix} \tau_L \\ \tau_R \end{bmatrix} = \begin{bmatrix} \tau_1 + \tau_2 \\ \tau_3 + \tau_4 \end{bmatrix} \quad (29)$$

where τ_L and τ_R denote the torques produced by the wheels on the left and right sides of the vehicle, respectively. Combining (26) and (27), this gives

$$F = B(q)\tau \quad (30)$$

where B is the input transformation matrix defined as:

$$B(q) = \frac{1}{2} \begin{bmatrix} \cos\theta & \cos\theta \\ \sin\theta & \sin\theta \\ -c & c \end{bmatrix} \quad (31)$$

Next, using (1), (23) and (30), the following dynamic model was obtained:

$$M(q)\ddot{q} + R(\dot{q}) = B(q)\tau \quad (32)$$

It should be noted that (30) describes the dynamics of a free body only and does not include the nonholonomic constraint (2). Therefore, a constraint had to be imposed on (30). To this end, a vector of Lagrange multipliers, λ , was introduced as follows:

$$M(q)\ddot{q} + R(\dot{q}) = B(q)\tau + A^T(q)\lambda \quad (33)$$

For control purposes it would be more suitable to express (29) in terms of the internal velocity vector η . Therefore, (33) was multiplied from the left by $S^T(q)$, which resulted in:

$$\begin{cases} S^T(q)M(q)\ddot{q} + S^T(q)R(\dot{q}) \\ = S(q)^T B(q)\tau + S^T(q)A^T(q)\lambda \end{cases} \quad (34)$$

After taking the time derivative of (3), this gave:

$$\ddot{q} = \dot{S}(q)\eta + S(q)\dot{\eta} \quad (35)$$

Next, using (33) and (3) in (31), the dynamic equations became

$$\bar{M}\dot{\eta} + \bar{C}\eta + \bar{R} = \bar{B}\tau \quad (36)$$

where

$$\bar{C} = S^T M \dot{S} = mx_{ICR} \begin{vmatrix} 0 & \dot{\theta} \\ \dot{\theta} & x_{ICR} \end{vmatrix} \quad (37)$$

$$\bar{M} = S^T M S = \begin{bmatrix} m & 0 \\ 0 & mx_{ICR}^2 + I \end{bmatrix} \quad (38)$$

$$\bar{R} = S^T R = \begin{bmatrix} F_{rx}(\dot{q}) \\ x_{ICR} F_{ry}(\dot{q}) + M_r \end{bmatrix} \quad (39)$$

$$\bar{B} = S^T B = \frac{1}{2} \begin{bmatrix} 1 & 1 \\ -c & c \end{bmatrix} \quad (40)$$

3.2. Hybridisation Controller Design for a Wheeled Mobile Robot

The principles and techniques of control theory are essential for the design, analysis, and optimization of feedback control systems to achieve the desired system behavior and performance. The control system could be standalone or hybridized based on the model complex. Individual control algorithms refer to standalone, single-technique control approaches, such as PID (proportional-integral-derivative) control, fuzzy logic control, adaptive control, optimal control, and robust control. They can be effective in handling specific types of control problems but may have limitations in handling more complex or uncertain systems. Individual control algorithms are generally simpler to design, implement, and tune compared to hybridized approaches. While hybridization can provide enhanced capabilities but at the cost of increased complexity, individual control algorithms offer a simpler and more targeted approach but may have limitations in handling certain control challenges. The choice between hybridization and individual control algorithms depends on the specific control problem, the desired performance characteristics, the complexity of the system, and the available resources for implementation and tuning. Hybridization can provide improved flexibility, robustness, and adaptability compared to individual control algorithms. The design of a hybrid control system requires more complexity to integrate the different components effectively. Hybridization is the combination of multiple control algorithms or techniques to achieve better performance or handle more complex systems. Hybridizing LQG with fuzzy control algorithms contributes to improved efficiency, increased driving range, enhanced regenerative braking, improved responsiveness and performance, flexibility in power management, increased reliability, and redundancy for wheeled mobiles for agricultural purposes. The goal of hybridizing LQG with fuzzy is to leverage the strengths of different control approaches and compensate for their individual weaknesses.

In the controller design, the first step is to design the linear quadratic regulator controller (Figure 5). If penalised gains from the LQR scenario are obtained, the penalised rate gain is identified. If not, go back to the LQR controller and adjust the penalised rate gain. If it is cheap, then the optimal gain values are passed to the fuzzy logic LQR controller framework. If not, then check whether an expensive penalised rate exists or not. If it is an expensive penalised rate, then the optimal gain values are passed to the fuzzy logic LQR controller framework. If not, it goes back to the LQR controller framework retuned. If the fuzzy logic LQR framework achieves the optimal penalisation rate, then it is optimised further and passed to the LQG framework. Based on the optimal gain, the LQG estimates the output parameters and adjusts the optimal gain in advance. After that, the greatest optimal controller gains are passed to the FLQG framework for its robust performance. Then, with wheeled mobile robot dynamics, the system is optimally regulated and robust.

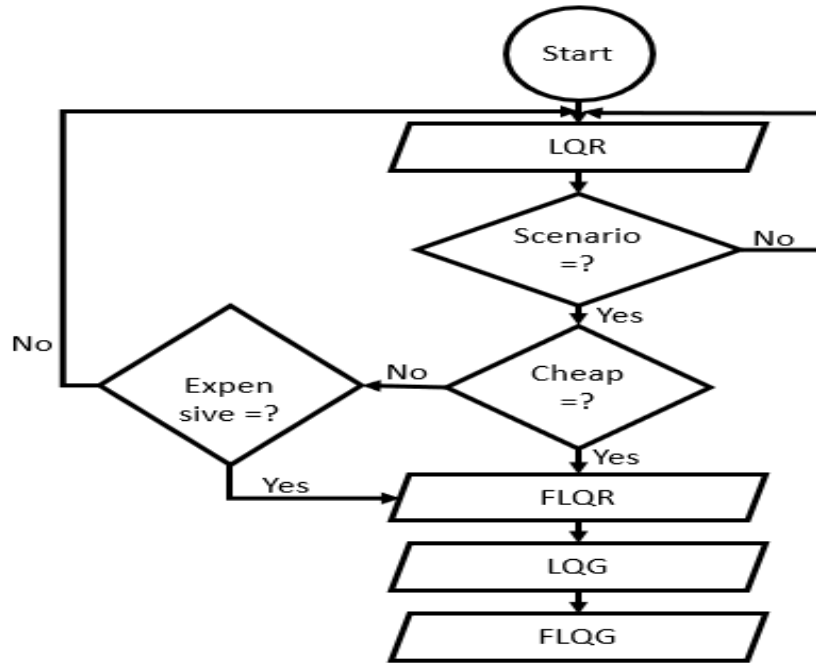


Figure 5. Fuzzy-LQG controller scheme.

The state feedback control (SFC) technique is based on the placement of the system poles. A gain matrix (K) and the state variables are used for the pole placement of the system. In SFC the poles of the closed-loop system may be placed in any chosen position. Nevertheless, for the methods of output feedback control, the poles of systems may be given to a definite point. In this technique, the state variables are implemented by a state feedback controller. The state variables of the system are feedback. All feedbacks multiplied by a state feedback gain matrix are compared with the reference input. The important point in the SFC design is to calculate K. The LQR controller is one of the most widely used methods for this. In the LQR controller, the optimal feedback parameters of the K matrix are taken by the cost function (J), which optimises the states, $x(t)$ and the control signal $u(t)$ of the system [8]:

$$u(t) = -Kx(t) \quad (41)$$

$$J = \frac{1}{2} \int_0^{+\infty} (x^T Q x + u^T R u) dt \quad (42)$$

J depends on the matrix Q and R. Q and R are defined as a positive semi-defined matrix. Furthermore, the K gain matrix is determined based on Q and R. The control signal is shown below:

$$u(t) = -R^{-1}B^T P(t)x = -Kx(t) \quad (43)$$

where P is obtained by the differential equation of Riccati:

$$PA + A^T - PBR^{-1}P + Q = 0 \quad (44)$$

The K matrix is determined with P. It is the solution of the Riccati equation:

$$K = R^{-1}B^T P = [k_1 \ k_2 \ k_3 \ \dots \ k_n] \quad (45)$$

n is the number of state variables. The LQR controller performance is dependent on the choice of weight matrices. In the literature, there are many different approaches for the choice of Q and R, for example Bryson's Rule. A simple choice approach can be $Q = I$ and $R = \rho I$. Furthermore, several optimisation algorithms can be used to obtain the optimal values of Q and R.

A. Fuzzy linear quadratic regulator (FLQR)

This controller is a combination of the optimal control approach (LQR) and the fuzzy control method. The fusion controller structure is used to design a linear fusion function (LFF). The LFF transforms the multiple variables into comprehensive error (E) and error change (EC), which simplifies the FLC controller. The FLC structure based on the LQR controller is illustrated in Figure 6.

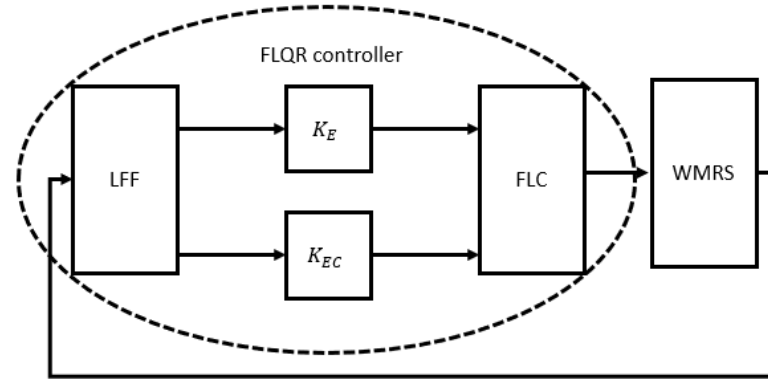


Figure 6. Block diagram of the FLQR controller in the WMRS system.

For the WMRS, the LFF is given as follows [33]:

$$F(x) = \begin{bmatrix} K_{\theta_1} & K_{\theta_2} & K_{\theta_3} & 0 & 0 \\ 0 & 0 & K_{\dot{\theta}_1} & K_{\dot{\theta}_2} & \end{bmatrix} \quad (46)$$

$$\begin{bmatrix} KR \\ KE \end{bmatrix} = F(X)x^T \quad (47)$$

$$\begin{cases} KR = K_{\theta_1} \theta_1 + K_{\theta_2} \theta_2 \\ KE = K_{\theta_1} \dot{\theta}_1 + K_{\theta_2} \dot{\theta}_2 \end{cases} \quad (48)$$

The Mamdani-type fuzzy model was developed with the aim of adjusting the closed-loop controller feedback gains. The input variables (KR and KE) and the output variable (Control signal-U) are converted into linguistic variables as follows: NB – negative big, NM – negative medium, NM – negative small, Z – zero, PS – positive small, PM – positive medium and PB – positive big. Triangular membership functions are used for the graphical inference of the input and output variables. Table 1 presents the fuzzy rules applied to the controller of the wheeled mobile robot [32].

Table 1. Fuzzy rules.

EC								
E	NB	NM	NS	ZE	PS	PM	PB	
NB	NB	NB	NB	NM	NM	NS	ZE	
NM	NB	NB	NM	NM	NS	ZE	PS	
NS	NB	NM	NM	NS	ZE	PS	PM	
ZE	NM	NM	NS	ZE	PS	PM	PM	
PS	NM	NS	ZE	PS	PM	PM	PB	
PM	NS	ZE	PS	PM	PM	PB	PB	
PB	ZE	PS	PM	PB	PB	PB	PB	

B. Linear quadratic Gaussian (LQG)

In a linear dynamic system, K_F estimates the system states from the information of input and output. Figure 7 shows the block diagram of the Kalman filter (K_F). Noised signals (W_d , W_n) are combined with the linear dynamic system to improve the system construction needed by the K_F algorithm.

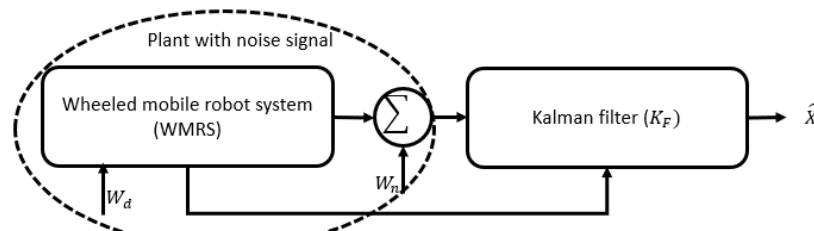


Figure 7. Block diagram of K_F .

According to the added noised signal, the state-space model of wheeled mobile robot can be the system given as follows [31]:

$$\begin{cases} \dot{X} = Ax + Bu + W_d \\ Y = Cx + Du + W_n \end{cases} \quad (49)$$

The dynamic equation of KF is added to the state space and is given by the equation [34]:

$$\begin{cases} \dot{\hat{X}} = A\hat{x} + Bu + K_f(y - \hat{y}) \\ Y = C\hat{x} \end{cases} \quad (50)$$

The K_F gain K_f is calculated as the follows:

$$K_f = PC^T R^{-1} \quad (51)$$

P and R are algebraic constants calculated with the Riccati equation and the output covariance matrix, respectively. \hat{x} and \hat{y} are the estimated state variables and outputs, respectively.

The error can be given:

$$e = \hat{x} - x \quad (52)$$

Using Eqs. (32) and (34), (35) is obtained.

$$\dot{e} = (A - k_f C)e \quad (53)$$

An optimal k_f gain matrix must be determined for the k_F design. The structure of LQG is taken by adding K_F to the LQR, as can be seen in Figure 9(b). The K_F is obligatory if the state variables of the LQR needed to be estimated. LQG is an optimal controller method for some systems that have uncertainty. The k_F is used to estimate the state variables according to the system input and the measured output variables. The state variables will be multiplied by the K matrix to generate the control signal (u):

$$u = -k\hat{x} \quad (54)$$

If the control signal is applied to the state-space model and the noise signals added to the system, the closed-loop model is given as follows:

$$\dot{x} = Ax - BK(x - \hat{x}) + W_d \quad (55)$$

The K_F state-space model is:

$$\dot{\varepsilon} = (A - K_f C)\varepsilon + W_d - K_f W_n \quad (56)$$

The new space model can be defined as:

$$\begin{bmatrix} \dot{x} \\ \dot{\varepsilon} \end{bmatrix} = \begin{bmatrix} (A - BK) & BK \\ 0 & (A - K_f C) \end{bmatrix} \begin{bmatrix} x \\ \varepsilon \end{bmatrix} + \begin{bmatrix} 1 & 0 \\ 1 & -K_f \end{bmatrix} \begin{bmatrix} W_d \\ W_n \end{bmatrix} \quad (57)$$

C. Fuzzy linear quadratic Gaussian controller (FLQG)

This FLQG controller structure is based on the combination of the LQG controller and FLQR controller. However, for certain cases, the state variables are not measured for real experimental systems. However, it is possible to estimate the non-measurable state by using the measurement data if the system is observable [25]. Furthermore, an estimation of state variables may be preferred because of the noisy measurement data. The structure of FLQG is obtained by adding the KF to the FLQR, as can be seen in Figure 8. However, the KF is obligatory if some state variables needed for the FLQR are estimated. KF estimates the state variables according to the DLRIP system input and the measured output variables. The estimated state variables are the input of the FLQR controller. A block diagram of FLQG controller is shown in Figure 8.

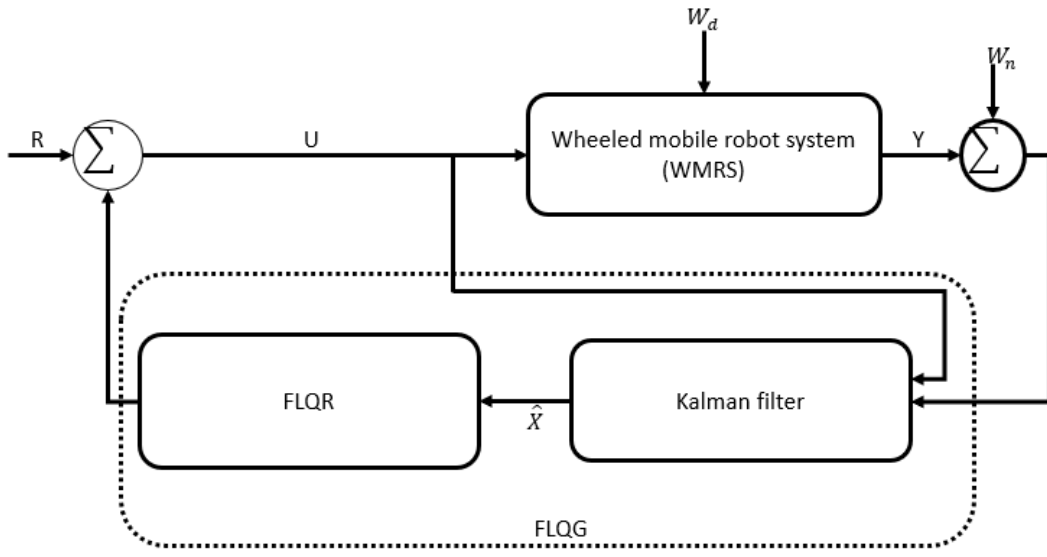


Figure 8. Block diagram of the FLQG controller for the wheeled mobile robot system.

Finally, the penalisation rate gains' numerical values were obtained, as shown in Table 2. The scenarios are cheap or expensive, and ignore any other state; they only interest one state. The penalisation rate of all linear quadratic regulators is positive, whereas linear quadratic Gaussian penalisation rates are positive diagonally, but are negative in the upper and lower matrices. These values suggest that some states are at the saddle point (see section 3.4) because LQG is sensitive to the dynamic nature of the WMRS. It is good that the wheeled mobile robot is stable at its core, but is still sensitive to very small changes in the dynamics system. The negative values in the penalisation rate indicated that the position and orientation responses are saddle points near zero. The positive penalisation rate indicated that all states are convergent in the region around zero.

Table 2. Results of penalisation rates.

Scenarios	Penalisation rate (KR)	Penalisation rate (KE)	Eigen values (E)
Cheap controller	[300.1181 111.8052]	$\begin{bmatrix} 100 & -100 \\ -100 & 2274500 \end{bmatrix}$	$\begin{bmatrix} -1152000 \\ -3700 \end{bmatrix}$
Expensive controller	[297.0804 110.9109]	$\begin{bmatrix} 100 & -100 \\ -100 & 2274500 \end{bmatrix}$	$\begin{bmatrix} -1133600 \\ -3700 \end{bmatrix}$
Ignore anyone state controller	[297.0804 111.0010]	$\begin{bmatrix} 100 & -100 \\ -100 & 2274500 \end{bmatrix}$	$\begin{bmatrix} -1135400 \\ -3700 \end{bmatrix}$

3.3. Hybridization Control Gain Design

This work determines an appropriate penalty rate gain, comprehends limits, and makes inferences in order to optimize controller design for agricultural drones. It creates a design method using fuzzy LQG control law, digitalizing classical LQG control law for use in contemporary applications, and controlling gain via feedback. Recalled equation (41) to equation (45)

$$t_{cmd} = K_R e(t) + K_E e(t) \quad (58)$$

where $e(t) = r(t) - y(t)$ is the tracking error signal between the reference $r(t)$ and the controlled system output, $y(t)$, and K_{E1}, K_{E2} are gains of LQG. This is first converted into the frequency domain to obtain

$$U(S)_{cmd} = K_R E(S) + K_E E(S) \quad (59)$$

and the associated Laplace transform is denoted by the capital variable. The bilinear transform can then be used to transfer this equation into the discrete-frequency domain with the variable z . Eliminating the denominator yields

$$U(Z)_{cmd} = K_R E(Z) + K_E E(Z) \quad (60)$$

A unique fuzzy logic version of Equation (...) will be developed for reliable system controllers, providing direct behavior insight and analytic structures for the easy prediction of actions, requiring good general rules. The fuzzy LQG control is developed from modern LQG. Based on the fuzzy control theory, the fuzzy relationship between the two LQG parameters (K_R and K_E) and the error e and error change rate e_z can be established. According to different e and e_z , the parameters (K_R and K_E) can be self-adjusted online in order to ensure that the controlled object has good dynamic and static performance, meeting different control requirements. In general, fuzzy control has no knowledge database, does not have adaptive ability, and its flexibility and interactivity are not very good. Contrarily, automatic-tuned systems often cannot be directly used to control objects or production processes. So, the combination of fuzzy LQG will bring their respective advantages into play.

$$e_z = Z_r - Z \quad (61)$$

Taking the time derivative for the above equation

$$\dot{e}_z = \dot{Z}_r - \dot{Z} \quad (62)$$

3.4. Dynamics of WMRS Characters Parameter Analysis

Settling time (T_s), i.e. the time required for the output to stabilise within a given tolerance band, is described mathematically as:

$$T_s = \begin{cases} \frac{4}{\sigma \omega_n}, & 0 < \sigma < 1 \\ \infty, & \sigma = 0 \\ \frac{6}{\omega_n}, & \sigma > 1 \end{cases} \quad (63)$$

where σ is the damping ratio.

Rise time (T_r) describes the time taken for the solution to increase from 0 % to 100 % of its ultimate value in under-damped systems, or from 10 % to 90 % of its final value in over-damped systems. Mathematically:

$$T_r = \frac{\pi - \theta}{\omega_d} \quad (64)$$

Peak time (T_p) is the time required for the response to reach the peak value for the first time. Mathematically:

$$T_p = \frac{\pi}{\omega_d} \quad (65)$$

Peak overshoot, or maximum overshoot (M_p), is defined as the deviation of the response at peak time from the final value of response. It is expressed as:

$$M_p = \left(e^{-\left(\frac{\sigma \pi}{\sqrt{1-\sigma^2}} \right)} \right) * 100 \quad (66)$$

At steady state time (T_{ss}), the rate of input is equal to the rate of elimination.

The RMS formula is defined as the square root of the mean (average) of the squares of the values in a dataset. In simpler terms, it calculates the average of the squared values and then takes the square root of that average. This process effectively converts the varying quantity into a single, representative value that reflects its overall magnitude:

$$RMS = \sqrt{\frac{1}{n} \sum_i x_i^2} \quad (67)$$

where RMS is the root mean square, n is the number of measurements from MATLAB simulation, and x_i is each state value of the WMRS dynamics system:

$$\% = \frac{\text{old value} - \text{new value}}{\text{old value}} * 100 \quad (68)$$

3.5. Lorenz System and Its Analyses for the WMRS Controller Framework

Based on the penalisation rate numerical values, it is necessary to look at the Lorenz law of attraction since, as reflected in Table 2, the values of the LQG are diagonally positive, but the upper and lower matrices are negative. It is therefore mandatory to relate them to the Lorenz law of attraction. The Lorenz law of attraction is considered a benchmark system in chaotic dynamics in that it displays extraordinary sensitivity to initial conditions and the strange attractor phenomenon. Even though the system tends to be stable, it is indeed possible to convert a strange attractor into a saddle point. Looking at the dynamics systems of WMRS after applying the controller's penalisation rate, the following implications were identified. In order to observe the controller behaviours, let $\dot{x} = f(x)$ near \hat{x} where $f(\hat{x}) = 0$. The dynamics systems of the WMRS were obtained with the expense and costs of linear quadratic Gaussian (LQG), because it made the dynamics system a saddle point. Zoom into fixed point, the dynamics of the position and orientation in a linear region can be seen. Let us assume

$$x = \hat{x} + \Delta x \quad (69)$$

$$\frac{d}{dt} \Delta x = \dot{x} = f(\hat{x} + \Delta x) = f(\hat{x}) + \frac{Df}{Dx}(\hat{x}) \cdot \Delta x + \frac{1}{2} \frac{D^2 f}{Dx^2}(\hat{x}) \cdot \Delta x^2 + \dots \quad (70)$$

Setting a higher order at zero, it gives:

$$\frac{1}{2} \frac{D^2 f}{Dx^2}(\hat{x}) \cdot \Delta x^2 + \dots = 0 \quad (71)$$

Then, $\frac{d}{dt} \Delta x \approx \frac{Df}{Dx}(\hat{x}) \cdot \Delta x \rightarrow \dot{x} = Ax$, $\frac{d}{dt} \Delta x = Ax$

$$x(t_0 + t) = e^{At} x(t_0) \quad (72)$$

$x = Tz \rightarrow \dot{z} = T^{-1} \dot{x} = T^{-1} ATz \rightarrow \dot{z} = \lambda z$ (diagonal decoupled system) $AT = T\lambda$.

where T is the eigen vector of the WMRS dynamics.

$$x(t) = T e^{\lambda t} T^{-1} x(0) \quad (73)$$

$$z(t) = T^{-1} x(0) \quad (74)$$

This means that if any initial condition $x(0)$ is taken, WMRS dynamics could be plotted in a time framework, showing how it would work with time using WMRS dynamics. $T^{-1} x(0)$ is taking the initial condition map into an eigen values coordinate system, where it is necessary to advance the system $\dot{z} = \lambda z$, that is $z(0)z(t)T e^{\lambda t}$. Now that the system is in the eigen value coordinate system, it should be mapped into the original equation (45). To strengthen the concept, consider the response of the WMRS, which is obtained from its dynamic equations [16]:

$$\begin{cases} x_r = x(t) \\ \dot{y}_r = rx(t) - y_r - x(t)z_r \\ \dot{z}_r = x(t)y_r - bz_r \end{cases} \quad (75)$$

The objective is to find:

$\{y_r(t) \rightarrow y(t)$ as $t \rightarrow \infty$. However, this approach does not work if z_r is replaced by $z(t)$.

$\{z_r(t) \rightarrow z(t)$

Taking into consideration the dynamics of the WMRS, let the errors of WMRS be:

$$\begin{cases} e_x = x - x_r \\ e_y = y - y_r \\ e_z = z - z_r \end{cases} \quad (76)$$

Then $e_x = 0$, $\dot{e}_y = \dot{y} - \dot{y}_r = -(y - y_r) - x(t)(z - z_r)$, where $e_y = y - y_r$, and $e_z = z - z_r$, which implies that

$$\dot{e}_y = e_y - x(t)e_z \quad (77)$$

$$\dot{e}_z = x(t)(y - y_r) - b(z - z_r) = x(t)e_y - be_z \quad (78)$$

$$\dot{e}_y e_y + \dot{e}_z e_z = -e_y^2 - x e_y e_z + x e_y e_z - b e_z^2 \quad (79)$$

$$\frac{d}{dt} \left(\frac{1}{2} (e_y^2 + e_z^2) \right) = -e_y^2 - b e_z^2 \quad (80)$$

Let

$$V = \frac{1}{2} (e_y^2 + e_z^2) \quad (81)$$

where V is a positive definite

$V = \frac{1}{2}(e_y^2 + e_z^2)\dot{V} < 0$ except at $(0,0)$, $V(t) \rightarrow 0 \Rightarrow e_y \rightarrow 0$, and $e_z \rightarrow 0$. This confirms that the WMRS dynamics system is stable.

4. Results and Discussion

If the wheeled mobile robot dynamics are not taken into consideration, the system is unstable throughout the time frame (Figure 9). Thus, to be stable the system needs regulation and a robust controller. The amplitude is very large, which shows that the system is skidding in space when it meets sudden impacts.

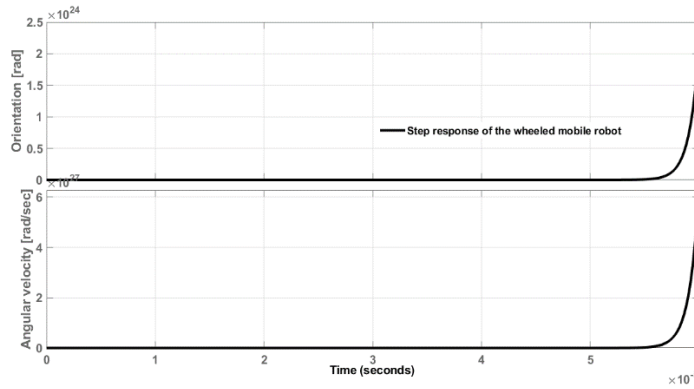


Figure 9. Step response without a controller.

Figure 10 shows the response of the WMRS for the step input with the inclusion of the linear quadratic Gaussian (LQG). The optimal penalised rate gains push the WMRS velocity forwards until it reaches the desired amplitude. However, the controller must exert a huge force in order to push the WMRS velocity. Since the WMRS model itself is nonlinear, there is a large area behind the plant responses. These areas indicate the amount of energy required to regulate the WMRS during the dynamic nature of WMRS. Even if it is optimally penalised, it needs more robust optimal penalised gains. This large area is due to the fact that LQG controllers can be sensitive to changes in the system dynamics, which can make them difficult to tune for optimal performance and can be computationally expensive. This is because LQG controllers require a significant amount of computation to calculate the optimal control inputs, which can be a problem for applications that have limited computational resources for WMRS.

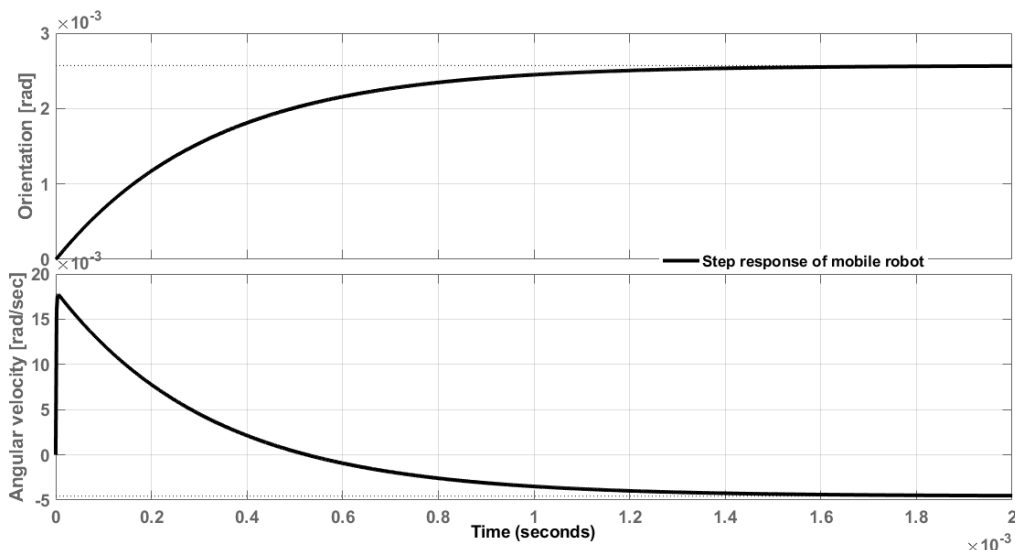


Figure 10. Step response for the LQG controller.

Figure 11 shows the response of the WMRS for the step input with the inclusion of the linear quadratic regulator (LQR). The optimal penalised rate gains push the WMRS velocity forwards until it reaches the desired amplitude. However, the controller must exert a huge force in order to push the WMRS velocity. The controller is very sensitive to the dynamics system since the WMRS model itself is a dynamics system. For this reason, there is a large area behind the plant responses. These areas indicate the amount of energy required to regulate the WMRS during the dynamic nature of WMRS. The more dynamic the system, the less LQR controller performance is obtained. Since LQR controllers assume that the system being controlled is linear, this assumption does not hold true for dynamics systems. In such cases, LQR controllers may not provide optimal performance or may even become unstable.

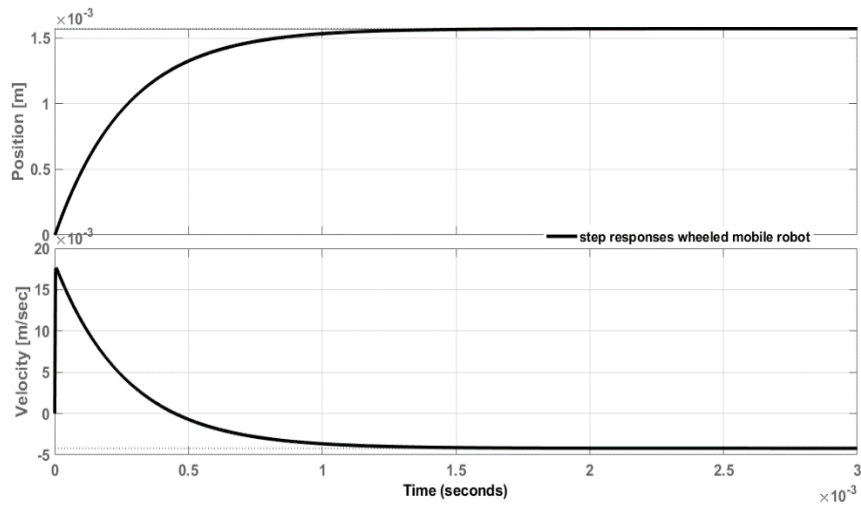


Figure 11. Step response for the LQR controller.

Certain types of controllers, such hybridized controllers used in vehicle control or industrial automation in agriculture, are made to function dependably in harsh environmental circumstances. A controller's performance, however, could be harmed by extremes in humidity, vibration, temperature, or other factors. Important things to think about are as follows:

4.1. Temperature Extremes

Elevated temperatures have the potential to overheat electronic components, resulting in decreased dependability and eventual malfunction. Very low temperatures can interfere with the functioning of electronic circuits and lead to problems with the mechanical parts of a mobile robot's wheel. In order to ensure optimal performance, hybridized controllers are frequently engineered with working temperature ranges, such as -20°C to 60°C.

4.2. Humidity and Moisture

Excessive humidity or moisture exposure can lead to condensation inside the controller enclosure, which can cause component degradation and short circuits. To stop the entry of water and dust, controllers with the proper ingress protection (IP) ratings are utilized. Internal components may be shielded with conformal coatings and desiccants.

4.3. Vibration and Shock

The controller's internal parts and connections may sustain mechanical damage as a result of strong vibrations or abrupt shocks. Rugged housings and shock-absorbing mountings are features of

controllers used in tough industrial environments or in wheeled mobile robot applications. Vibration problems are less common in solid-state architectures since they lack moving elements.

4.4. Power Fluctuations

Brownouts, spikes in voltage, or total power outages can cause component damage and interfere with the controller's ability to function. In order to continue operating during brief power outages, controllers frequently include backup power sources and power conditioning built right in.

In order to guarantee dependable functioning in harsh circumstances, hybridized controllers usually:

- Designed with components and materials rated for the expected environmental stresses
- Housed in rugged, sealed enclosures to protect internal electronics
- Programmed with failsafe mechanisms and fault-tolerant control algorithms
- Regularly tested and maintained to identify and address any degradation in performance

Because of their strong construction and advanced control techniques, well-designed hybridized (Fuzzy-LQG) controllers can continue to operate efficiently even under the most adverse conditions.

Figure 12 shows the performance of the hybridised controller. The response of the WMRS is stable without much energy loss. However, after some time, the controller effort increases negatively. This means that the controller's effort is heavily penalised in order to achieve robust stability during dynamic motion. Owing to this, the plant's response becomes robustly stable with a small amount of energy loss. It can be carefully observed from Figure 12 that after 20 seconds, the WMRS position and velocity shifted a little and remained stable throughout the numerical values. This is because the WMRS is no longer stable around zero, but instead stable in some numerical value region. In short, the region of convergence is not around zero. Due to the linear quadratic Gaussian (LQG) control design of the upper and lower matrices, the penalisation rate is negative, which can lead to instability in the minor system (products of both velocity and position). Negative gain values in the LQG controller can cause the system to exhibit undesirable behaviours such as oscillations, divergence or uncontrollable responses in the upper and lower matrices, but the effect is minor since the upper and lower matrices are obtained as the product of two states. Consequently, it leads to a saddle point, a region in which the states have dual properties (the state of convergence and the state of divergence).

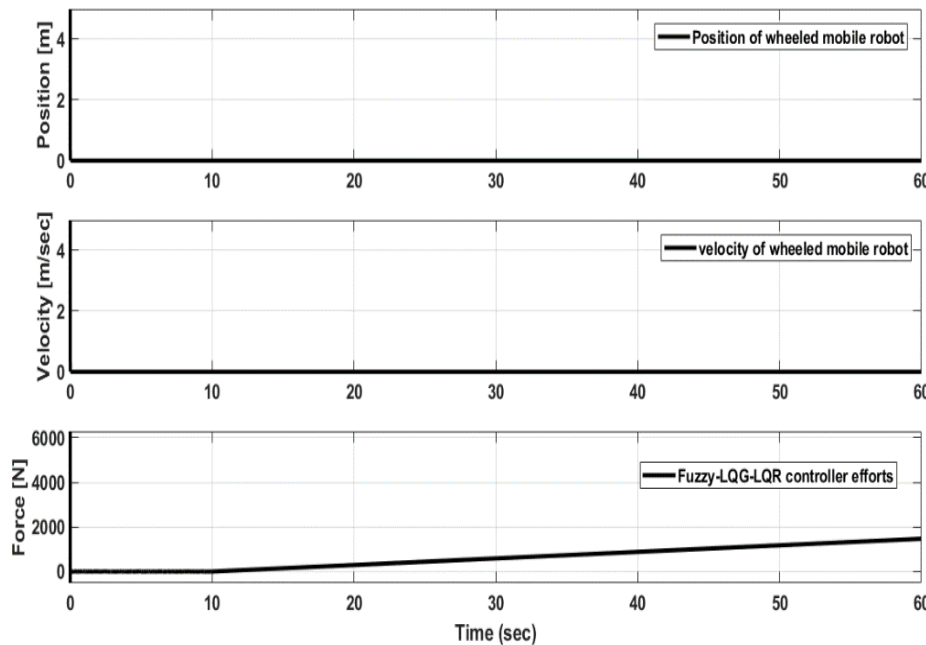


Figure 12. Cheap penalisation rate for linear motion.

The orientation and angular velocity of the WMRS are shown in Figure 13. Both orientation and angular velocities are effectively stable at a given controller effort. The controller effort is increasing due to the dynamic nature of the WMRS. Even if the controller gains are cheap, they could be robustly stabilised throughout the entire orientation and angular velocity. Thus, the cheap controller scenarios are more effective for the WMRS dynamics system.

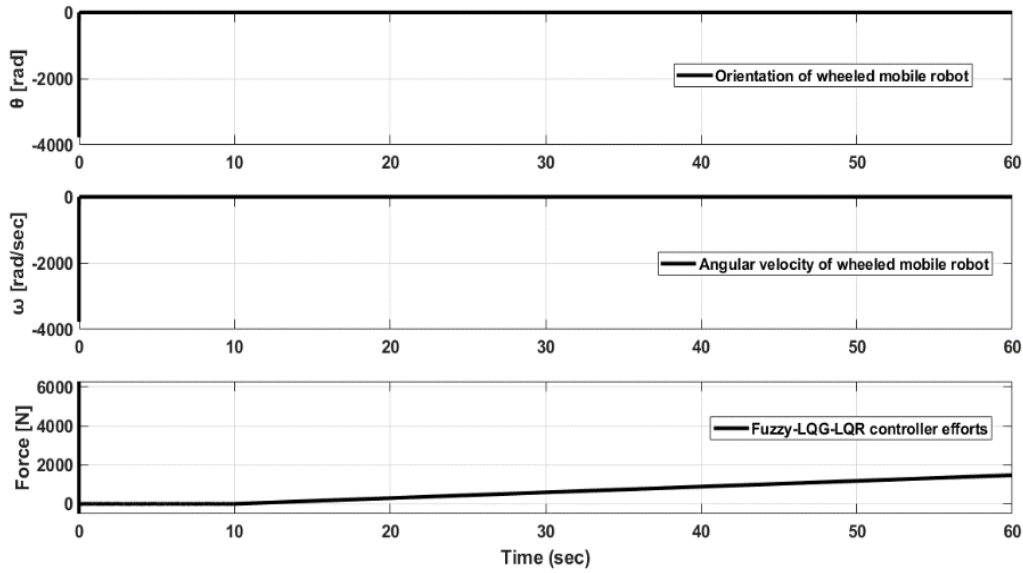


Figure 13. Cheap penalisation rate for angular motion.

Initially, the WMRS response increases until it reaches zero, then remains stable throughout the period (Figure 14). Owing to the expensiveness of the controller gains, the response of the WMRS is stable without overshoot. The good news is the controller expensiveness, which makes the penalisation rate gain a non-zero, and it increases positively since the WMRS is in dynamic conditions.

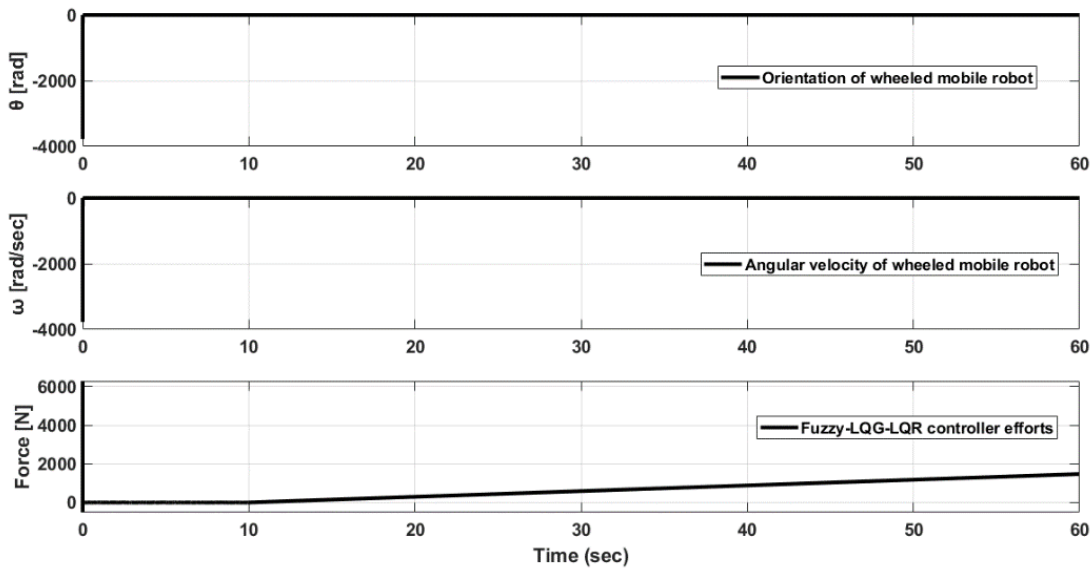


Figure 14. Expensive penalisation rate for angular motion.

As the WMRS response approaches zero, it falls until it stabilises for the duration of the observation (Figure 15). The WMRS response is stable and free of overshoot due to the high cost of

the controller improvements. As the controller is costly and the WMRS operates in dynamic situations, the WMRS response is easily steady. The stability was granted with the expense and costs of innermost controller gains (LQG and LQR). The controllers allow the state to be zero for the whole time, but the benefit is that the controller is trying to stabilise all the states, regardless of the dynamics of the WMRS, which is why the controller gains non-zero and positive values the whole time.

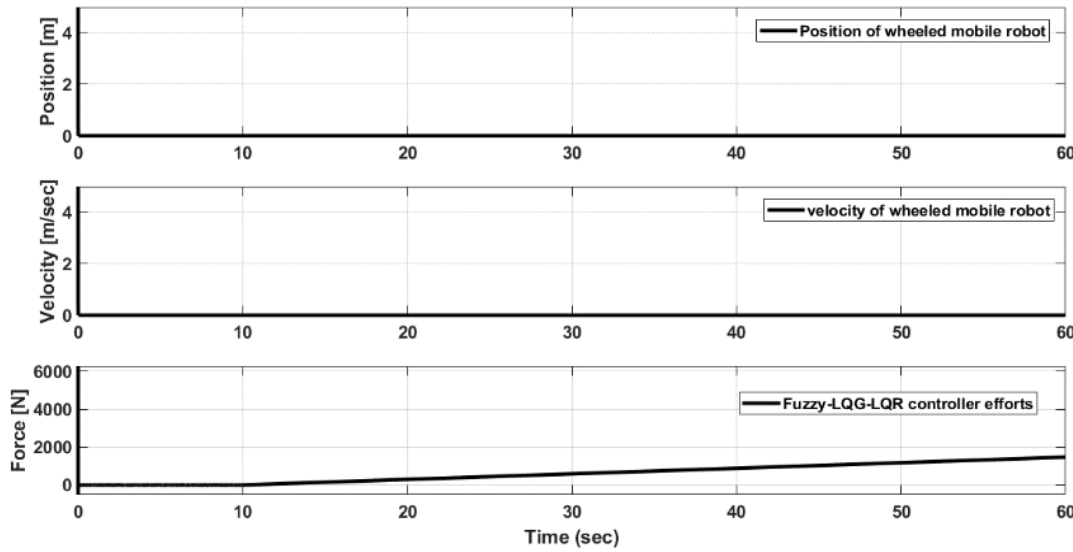


Figure 15. Expensive penalisation rate for linear motion.

This study expands the LQR (linear quadratic regulator, solved by optimisation), LQG (linear quadratic Gaussian), and fuzzy logic controllers to create an estimate of the states when fewer measurements are available (and yet observable) for the WMRS estimators. If the states are stable, then the estimate for the states approaches the state values. The combination of LQR and LQG results in a controller that can be optimised to find these parameters independently, at least without the effect of noise or disturbances. If these optimised penalisation rates are passed to the fuzzy logic controllers, the fuzzy logic controller is made more robust by the system. After applying the entire system to WMRS internally, the innermost controller gains are sensitive and easily exposed to the dynamics system. To make this clearer, the Lorenz law of attractions is applied, which is obtained based on the application of the penalisation rate to the system. The position of the WMRS is demonstrated in Figure 16. The position was zoomed in on the x and y axes in order to understand the nature of the WMRS dynamics system. It has been predicted that the position of the wheeled mobile robot system will experience saddle points near zero. Around the zero (saddle) points there are often optimisation problems in WMRS, but they can be used to identify potential solutions. For example, in the case of WMRS dynamic variables, a saddle point can be used to identify a point where the WMRS dynamic is neither a maximum nor a minimum, but instead is a point of inflection. The saddle points develop because the upper and lower matrices are negative; however, the controller gains push the state to a stable region. These show the robustness of a combination of the three controllers (LQR, LQG and fuzzy logic) applied to WMRS, where the states of WMRS can be stabilised.

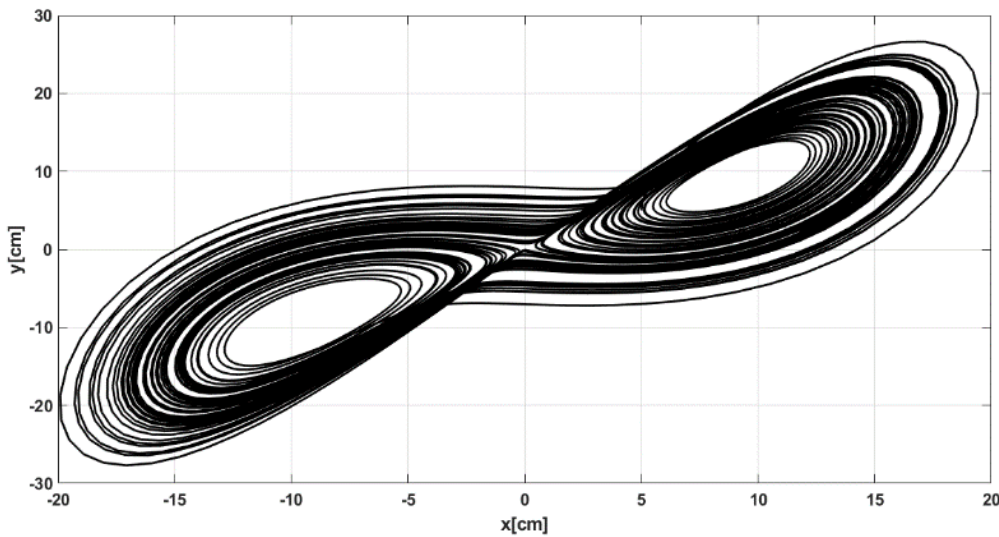


Figure 16. Lorenz attraction for the WMRS position along the x and y axes.

The position of the WMRS dynamics system was zoomed in on the x and z axes in order to understand the nature of the WMRS system (Figure 17) on the x and z axes. Around zero, the dynamic state of the WMRS becomes critical. The fact that this happens means that the inner (LQR and LQG) controllers are sensitive to very small changes in the dynamics of WMRS, and that in a dynamic system of WMRS, a critical point is a point where the WMRS system's state does not change over time. However, the penalised rate gains obtained are trying to push the states near the region of convergence (stable).

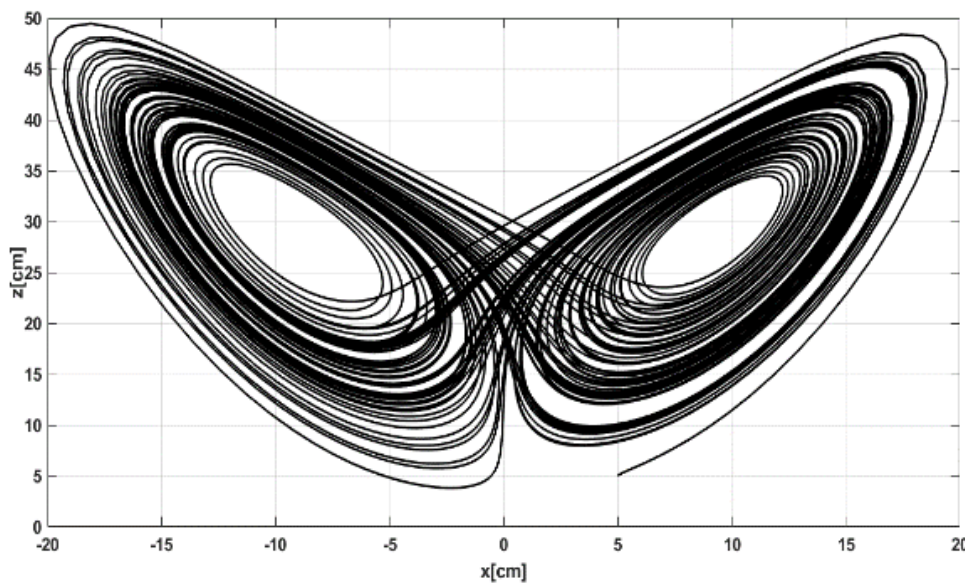


Figure 17. Lorenz attraction for the WMRS position along the x and z axes.

To comprehend the nature of the WMRS system, the position of the WMRS dynamics system was magnified on the y and z axes (Figure 18). This point implies that the WMR system's behaviour changes from stable to unstable. The WMRS dynamic state reach a crucial point at about zero. Since then, extremely slight variations in the WMRS dynamics cause the LQR and LQG controllers to become sensitive. This implies that a critical point in a dynamical WMRS system is a point at which the state of the WMRS system remains constant across time.

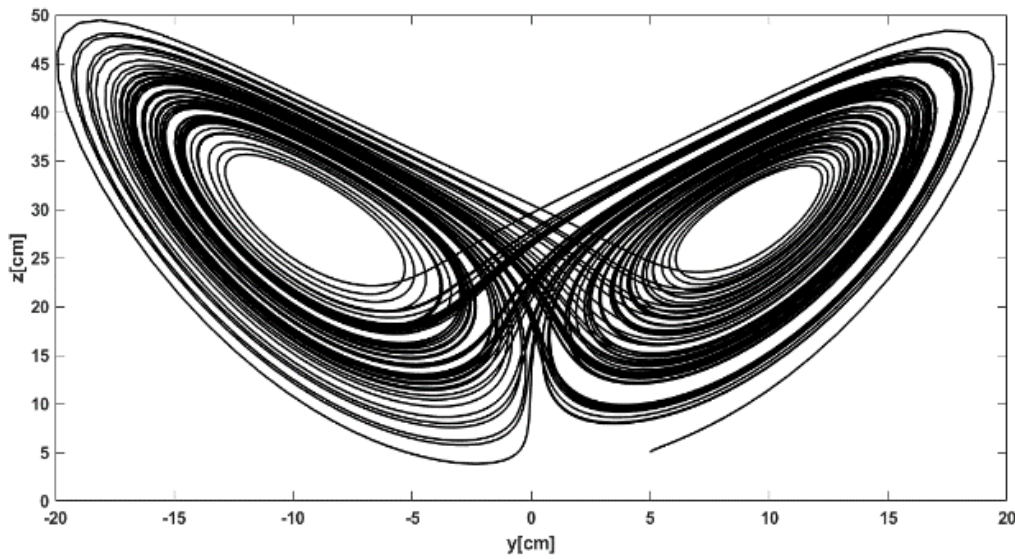


Figure 18. Lorenz attraction for the WMRS position along the y and z axes.

Table 3 shows the WMRS parameters characteristic for the respective controllers. The steady state error performance of FLQG over both LQR and LQG is 99.77 % and 99.76 %, respectively. The peak amplitude performance of FLQG is 77% over LQR, and 76.9 % over LQG. The settling time response by FLQG is 87.2 % over LQR, and 87.1 % over LQG whereas the rise time response of FLQG over LQR and LQG is 68.8 % for both.

Table 3. Characteristics of WMRS parameters.

Specifications	Error by LQR	Error by LQG	Error by FLQG	%FLQG over LQR	%FLQG over LQG
Steady state error [%]	0.001	0.000998	0.0000023	99.77	99.76
Peak amplitude [m/sec]	0.1	0.0998	0.023	77	76.9
Settling time [sec]	0.782	0.781	0.1	87.2	87.1
Rise time [sec]	0.439	0.439	0.137	68.8	68.8
Overshoot [%]	0	0	0	0	0

Table 4 shows the simulation results of Rms for FLQG cheap control and for FLQG expensive control.

Table 4. WMRS response at different input parameters.

Parameters	Error FLQG cheap control				Error FLQG expensive control			
	Position [cm]	Orientation [rad]	Velocity [m/sec]	Angular velocity [rad/sec]	Position [cm]	Orientation [rad]	Velocity [m/sec]	Angular velocity [rad/sec]
Step input	0.3493	0.3498	0.02088	0.02088	0.0006608	0.0006642	0.0005642	0.0005642
Double pulse input	0.3493	0.3498	0.02088	0.02088	0.0006608	0.0006642	0.0005642	0.0005642
Square input	0.3493	0.3498	0.02088	0.02088	0.0006608	0.0006642	0.0005642	0.0005642

In a quantitative comparison of the performance of previous (FLQG) and current (FLQG) controllers under external disturbances, the steady state error improvements in the current work compared with the previous work were 99.97 % better, whereas peak amplitude improvements were 71.25 % better than the previous work (Table 5). The settling time of the current work is a 99.6 % improvement over the previous work with the same controller algorithms.

Table 5. Quantitative comparison of the previous work and current work.

Specifications	FLQG [37]	FLQG	%FLQG over FLQG [37]
Steady state error [%]	0.01	0.0000023	99.97
Peak amplitude [%]	0.08	0.023	71.25
Settling time [sec]	23.75	0.1	99.6

5. Conclusions

In this paper, the dynamics models of a wheeled mobile were developed and its controller designed. The controllers were hybridised (linear quadratic regulator, linear quadratic Gaussian and fuzzy logic) controllers, since controllers share their good qualities in order to make robust responses to the WMRS dynamics. The frameworks of the proposed controllers were verified using Lorenz's law of attraction. In terms of controller performance, the LQR controller played a greater role in stabilising the WMRS dynamics system since it was considered the innermost loop. Based on the LQR controller penalisation rate, LQG estimated the dynamic nature of the WMRS. After effectively estimating the dynamic states of the WMRS fuzzy logic controller, it activated its membership function. Based on this controller performance, the dynamic of the WMRS is robustly stable and regulated. From these results, it is inferred that the response of the position was stable at saddle points (near zero), whereas the velocity of the WMRS was fully stable near zero. This occurred because of the nature of the LQR and LQG controllers. These controllers are very sensitive to small changes in state dynamics. However, they were later adjusted by fuzzy logic controllers. The settling time response by FLQG was 87.2 % over LQR, and 87.1 % over LQG, whereas the rise time responses of FLQG over both LQR and LQG were both 68.8 %. This implies that hybridisation controllers were more effective for WMRS dynamics. Rms FLQG for cheap control was 0.3493 cm and 0.3493 rad in position and orientation, respectively. A velocity response of 0.02088 m/sec and angular velocity response of 0.02088 rad/sec errors FLQG were obtained by applying cheap controller scenarios, whereas for expensive control the responses errors for position and orientation were 0.0006608 cm and 0.0006642 rad respectively, and the velocity responses error were 0.0005642 m/sec and angular velocity response error 0.0005642 rad/sec. For this performance, the WMRS was stable and well regulated, therefore the proposed controller is excellent for the WMRS system dynamics in agricultural applications.

Authors' Contributions: Conceptualization, Sairoel Amertet Finecomess and Girma Gebresenbet; Methodology, Sairoel Amertet Finecomess; Software, Sairoel Amertet Finecomess; Validation, Sairoel Amertet Finecomess; Formal analysis, Sairoel Amertet Finecomess; Investigation, Sairoel Amertet Finecomess; Resources, Sairoel Amertet Finecomess; Data curation, Sairoel Amertet Finecomess; Writing – original draft, Sairoel Amertet Finecomess, Girma Gebresenbet and Hassan Mohammed Alwan; Writing – review & editing, Sairoel Amertet Finecomess and Hassan Mohammed Alwan; Visualization, Sairoel Amertet Finecomess; Supervision, Girma Gebresenbet and Hassan Mohammed Alwan; Project administration, Girma Gebresenbet; Funding acquisition, Girma Gebresenbet.

Funding: This research received no external funding.

Availability of Supporting Data: The data presented in this study are available in article.

Acknowledgments: we acknowledgment Uppsala university, Sweden, and saint Peterburg poly technique university, Russia.

Conflict of interests: The authors declare no conflict of interest.

Reference

1. S. Amertet, G. Gebresenbet, H. M. Alwan, and K. O. Vladmirovna, "Assessment of Smart Mechatronics Applications in Agriculture: A Review," *Appl. Sci.*, vol. 13, no. 12, p. 7315, 2023.
2. M. Faiz, B. Sumantri, and B. S. B. Dewantara, "Double Loop Controller of Four Mecanum-Wheel Automated Guided Vehicle using SMC-PID," in *2023 International Electronics Symposium (IES)*, IEEE, 2023, pp. 305–310. Accessed: Feb. 11, 2024. [Online]. Available: <https://ieeexplore.ieee.org/abstract/document/10242526/>
3. R. Shamshiri and W. I. Wan Ishak, "Design and simulation of control systems for a field survey mobile robot platform," *Res. J. Appl. Sci. Eng. Technol.*, vol. 6, no. 13, pp. 2307–2315, 2013.

4. G. An *et al.*, "EASS: An automatic steering system for agricultural wheeled vehicles using fuzzy control," *Comput. Electron. Agric.*, vol. 217, p. 108544, 2024.
5. C. Luo *et al.*, "Design and Evaluation of Field Segmentation, Path Generation and Sequential Point Tracking Algorithms for Agricultural Mobile Robots," *J. ASABE*, p. 0, 2024.
6. H. Yoo, D. Baek, and S. Choi, "Navigation Path Following Platform for a Greenhouse Shuttle Robot Using the State-flow Method," *Math. Probl. Eng.*, vol. 2024, 2024, Accessed: Feb. 25, 2024. [Online]. Available: <https://www.hindawi.com/journals/mpe/2024/8810990/>
7. H. Kang, C.-W. Park, and C.-H. Hyun, "Alternative identification of wheeled mobile robots with skidding and slipping," *Int. J. Control. Autom. Syst.*, vol. 14, no. 4, pp. 1055–1062, Aug. 2016, doi: 10.1007/s12555-015-0095-y.
8. S. Amertet, G. Gebresenbet, and H. M. Alwan, "Optimizing the performance of a wheeled mobile robots for use in agriculture using a linear-quadratic regulator," *Robot. Auton. Syst.*, p. 104642, 2024.
9. L. Emmi, R. Fernández, and P. Gonzalez-de-Santos, "An Efficient Guiding Manager for Ground Mobile Robots in Agriculture," *Robotics*, vol. 13, no. 1, p. 6, 2023.
10. R. Shamshiri and W. I. W. Ismail, "Control system design for a field survey agricultural mobile robot," in *International Conference on Agricultural and Food Engineering for Life (Cafei2012)*, 2012, p. 28. Accessed: Feb. 11, 2024. [Online]. Available: https://www.researchgate.net/profile/Redmond-Shamshiri/publication/280093083_Control_System_Design_for_a_Field-Survey_Agricultural_Mobile_Robot/links/55a8467e08aea994671dd8b5/Control-System-Design-for-a-Field-Survey-Agricultural-Mobile-Robot.pdf
11. R. Cale, "Modeling and Control of a Four-wheel Autonomous Agricultural Robot," Master's Thesis, NTNU, 2021. Accessed: Feb. 11, 2024. [Online]. Available: <https://ntnuopen.ntnu.no/ntnu-xmlui/bitstream/handle/11250/2787895/no.ntnu:inspera:76427839:20997435.pdf?sequence=1>
12. X. Tu, "Robust navigation control and headland turning optimization of agricultural vehicles," PhD Thesis, Iowa State University, 2013. Accessed: Feb. 25, 2024. [Online]. Available: <https://search.proquest.com/openview/2e57452e00a58cd99d9cb79572008df4/1?pq-origsite=gscholar&cbl=18750>
13. X. Li and M. Wang, "Consensus control for wheeled mobile robots under input saturation constraint," *IEEE Access*, vol. 8, pp. 177125–177130, 2020.
14. C. Moon and W. Chung, "Kinodynamic planner dual-tree RRT (DT-RRT) for two-wheeled mobile robots using the rapidly exploring random tree," *IEEE Trans. Ind. Electron.*, vol. 62, no. 2, pp. 1080–1090, 2014.
15. H. Yang, X. Fan, P. Shi, and C. Hua, "Nonlinear control for tracking and obstacle avoidance of a wheeled mobile robot with nonholonomic constraint," *IEEE Trans. Control Syst. Technol.*, vol. 24, no. 2, pp. 741–746, 2015.
16. S. Ryu, J. Won, H. Chae, H. S. Kim, and T. Seo, "Evaluation Criterion of Wheeled Mobile Robotic Platforms on Grounds: A Survey," *Int. J. Precis. Eng. Manuf.*, vol. 25, no. 3, pp. 675–686, Mar. 2024, doi: 10.1007/s12541-023-00912-6.
17. S. Kamon *et al.*, "Energy Consumption of a Wheel/Track Reconfigurable Mobile Robot on the Farm," in *2024 IEEE/SICE International Symposium on System Integration (SII)*, IEEE, 2024, pp. 798–803. Accessed: Feb. 25, 2024. [Online]. Available: <https://ieeexplore.ieee.org/abstract/document/10417300/>
18. D. A. V. Trinh and N. T. Thinh, "A Study of an Agricultural Indoor Robot for Harvesting Edible Bird Nests in Vietnam," *AgriEngineering*, vol. 6, no. 1, pp. 113–134, 2024.
19. J. Qu, Z. Zhang, Z. Qin, K. Guo, and D. Li, "Applications of Key Autonomous Navigation Technologies for Unmanned Agricultural Tractors: A Review," 2024, Accessed: Feb. 25, 2024. [Online]. Available: <https://www.preprints.org/manuscript/202402.0401>
20. W. Yuan, Y. Liu, Y.-H. Liu, and C.-Y. Su, "Differential flatness-based adaptive robust tracking control for wheeled mobile robots with slippage disturbances," *ISA Trans.*, vol. 144, pp. 482–489, 2024.
21. K. Wang, Z. Xu, K. Zhang, Y. Huang, and J. Xu, "Lattice piecewise affine approximation of explicit nonlinear model predictive control with application to trajectory tracking of mobile robot," *IET Control Theory Appl.*, vol. 18, no. 2, pp. 149–159, Jan. 2024, doi: 10.1049/cth2.12553.
22. A. Mehallel, L. Mérida-Calvo, R. Rivas-Perez, and V. Feliu-Batlle, "A New Smith Predictor Motor Control System to Reduce Disturbance Effects Caused by Unknown Terrain Slopes in Mobile Robots," in *Actuators*, MDPI, 2024, p. 46. Accessed: Feb. 25, 2024. [Online]. Available: <https://www.mdpi.com/2076-0825/13/2/46>

23. D. Dirckx, M. Bos, B. Vandewal, L. Vanroye, W. Decré, and J. Swevers, "ASAP-MPC: An Asynchronous Update Scheme for Online Motion Planning with Nonlinear Model Predictive Control." arXiv, Feb. 09, 2024. Accessed: Feb. 25, 2024. [Online]. Available: <http://arxiv.org/abs/2402.06263>
24. M. Ahsan and M. M. Salah, "Improved nonlinear model predictive control with inequality constraints using particle filtering for nonlinear and highly coupled dynamical systems," *Nonlinear Eng.*, vol. 13, no. 1, p. 20220351, Feb. 2024, doi: 10.1515/nleng-2022-0351.
25. O. Y. Ismael, M. Almaged, and A. I. Abdulla, "Nonlinear Model Predictive Control-based Collision Avoidance for Mobile Robot," *J. Robot. Control JRC*, vol. 5, no. 1, pp. 142–151, 2024.
26. Y. Tang, S. Qi, L. Zhu, X. Zhuo, Y. Zhang, and F. Meng, "Obstacle Avoidance Motion in Mobile Robotics," *J. Syst. Simul.*, vol. 36, no. 1, p. 1, 2024.
27. Y. Zheng, J. Zheng, K. Shao, H. Zhao, H. Xie, and H. Wang, "Adaptive trajectory tracking control for nonholonomic wheeled mobile robots: A barrier function sliding mode approach," *IEEECAA J. Autom. Sin.*, 2024, Accessed: Feb. 25, 2024. [Online]. Available: <https://ieeexplore.ieee.org/abstract/document/10379559/>
28. Y. Zheng, J. Zheng, K. Shao, H. Zhao, Z. Man, and Z. Sun, "Adaptive fuzzy sliding mode control of uncertain nonholonomic wheeled mobile robot with external disturbance and actuator saturation," *Inf. Sci.*, p. 120303, 2024.
29. T. Zhao, P. Qin, S. Dian, and B. Guo, "Fractional order sliding mode control for an omni-directional mobile robot based on self-organizing interval type-2 fuzzy neural network," *Inf. Sci.*, vol. 654, p. 119819, 2024.
30. M. Y. Silaa, A. Bencherif, and O. Barambones, "Indirect Adaptive Control Using Neural Network and Discrete Extended Kalman Filter for Wheeled Mobile Robot," in *Actuators*, MDPI, 2024, p. 51. Accessed: Feb. 25, 2024. [Online]. Available: <https://www.mdpi.com/2076-0825/13/2/51>
31. M. Rybczak, N. Popowniak, and A. Lazarowska, "A Survey of Machine Learning Approaches for Mobile Robot Control," *Robotics*, vol. 13, no. 1, p. 12, 2024.
32. R. S. Patil, S. P. Jadhav, and M. D. Patil, "Review of Intelligent and Nature-Inspired Algorithms-Based Methods for Tuning PID Controllers in Industrial Applications," *J. Robot. Control JRC*, vol. 5, no. 2, pp. 336–358, 2024.
33. A. A. Nada and M. A. Bayoumi, "Development of embedded fuzzy control using reconfigurable FPGA technology," *Automatika*, vol. 65, no. 2, pp. 609–626, Apr. 2024, doi: 10.1080/00051144.2024.2313904.
34. F. Zafar *et al.*, "Stabilization and tracking control of underactuated ball and beam system using metaheuristic optimization based TID-F and PIDD2-PI control schemes," *Plos One*, vol. 19, no. 2, p. e0298624, 2024.
35. C. Li, C. Ma, Y.-H. Chen, and R. Yu, "Stratified Game-Theoretic Optimization of Robust Control Design for Fuzzy Dynamical Systems: A Hybrid Nash–Stackelberg Strategy," *IEEE Trans. Syst. Man Cybern. Syst.*, 2024, Accessed: Feb. 25, 2024. [Online]. Available: <https://ieeexplore.ieee.org/abstract/document/10384797/>
36. T. V. A. Nguyen and N. H. Tran, "A TS Fuzzy Approach with Extended LMI Conditions for Inverted Pendulum on a Cart," *Eng. Technol. Appl. Sci. Res.*, vol. 14, no. 1, pp. 12670–12675, 2024.
37. "Development of a Fuzzy-LQR and Fuzzy-LQG stability... - Google Scholar." Accessed: Feb. 25, 2024. [Online]. Available: https://scholar.google.com/scholar?hl=en&as_sdt=0%2C5&as_ylo=2024&scioq=Optimizing+the+performance+of+a+wheeled+mobile+robots+for+use+in+agriculture+using+a+linear-quadratic+regulator&q=Development+of+a+Fuzzy-LQR+and+Fuzzy-LQG+stability+control+for+a+double+link+rotary+inverted+pendulum&btnG=

Disclaimer/Publisher's Note: The statements, opinions and data contained in all publications are solely those of the individual author(s) and contributor(s) and not of MDPI and/or the editor(s). MDPI and/or the editor(s) disclaim responsibility for any injury to people or property resulting from any ideas, methods, instructions or products referred to in the content.